Modulated superconductivity due to vacancy and magnetic order in $A_y\mathrm{Fe}_{2-x/2}\mathrm{Se}_2$ [A = Cs, K, (Tl,Rb), (Tl,K)] iron-selenide superconductors

Tanmoy Das[1] and A. V. Balatsky[1,2]

[1]*Theoretical Division, Los Alamos National Laboratory, Los Alamos, New Mexico 87545, USA*

[2]*Center for Integrated Nanotechnologies, Los Alamos National Laboratory, Los Alamos, New Mexico 87545, USA*

We present a calculation of a "modulated" superconducting state in iron-selenide superconductors. The zero-momentum d-wave pairing breaks the translational symmetry of the conventional $\mathrm{BaFe}_2\mathrm{Se}_2$-like crystal of the $I4/mmm$ space group. This pairing state becomes compatible when the Fe vacancies form an ordered state and the crystal symmetry changes to a low-temperature $I4/m$ one. For the specific case of an incommensurate vacancy order at $Q_v = (\frac{1}{5}, \frac{3}{5})$ in $\mathrm{K}_{0.82(2)}\mathrm{Fe}_{1.626(3)}\mathrm{Se}_2$, we find that it induces a block checkerboard antiferromagnetic phase at wave vector $\mathbf{Q}_m = 4\mathbf{Q}_v$. The coexistence of vacancy order and magnetic order leads to a reconstructed ground state which naturally couples to the d-wave superconductivity in a uniform phase in what we propose will be a general coupling for all iron-selenide superconductors. Our results agree with numerous experimental data available to date. We thus suggest that the incommensurability leads to a uniform coexistence of multiple phases as a viable alternative to a nanoscale phase separation in high-T_c superconductors and play an important role in the enhancement of superconductivity.

I. INTRODUCTION

The layered iron-selenide compounds $A_y\mathrm{Fe}_{2-x/2}\mathrm{Se}_2$ [A = Cs, K, (Tl,Rb), (Tl,K)] have been found recently to become superconducting (SC) with highest $T_c \sim 32$ K when a suitable value of the Fe vacancy concentration $x \sim 0.87$ is achieved.[1] This fascinating tunability of the SC property with Fe vacancy has opened up a new platform to study the mechanism of unconventional superconductivity. Most interestingly, the onset of vacancy order is accompanied by several interesting changes of the structural, electronic, magnetic, and SC properties. In particular, numerous experiments have found that the superconductivity turns on exactly when the randomly placed Fe vacancies also form an ordered state in addition to a structural phase transition.[2] Simultaneously, the value of the magnetic moment is dramatically enhanced on each Fe site.[2]

We show here that in these materials the vacancy order induces the magnetic order, and that both phases uniformly coexist with d-wave superconductivity to lead to a "modulated superconductor." The induction of a modulated order due to the incommensurability of another, competing, order is a common phenomenon in unconventional superconductors. Historically the incommensurate spin-density wave (SDW) order in cuprates was first found in neutron scattering experiment $\mathrm{La}_{1.6-x}\mathrm{Nd}_{0.4}\mathrm{Sr}_x\mathrm{CuO}_4$ with wave vector $Q_m = (\pi \pm \delta, \pi)/(\pi, \pi \pm \delta)$,[3] similar to the case of Cr.[4] Subsequently, an induced charge density wave (CDW) order at $Q_c = (2\delta, 0)/(0, 2\delta)$ is also measured in scanning tunneling microscopy (STM).[5,6] The coexistence of SDW and CDW produces a "stripe"-like pattern in cuprates which is observed by neutron scattering and angle-resolved photoemission spectroscopy (ARPES) in La-based cuprates, STM in $\mathrm{Bi}_2\mathrm{Sr}_2\mathrm{CuO}_{6+\delta}$ (Bi2201) and quantum oscillations, and Nernst signal and Seeback measurements in YBCO families.[7–9] Similarly, in iron-pnictides ($\mathrm{BaFe}_2\mathrm{As}_2$) and chalcogenides ($\mathrm{FeTe}_{1-x}\mathrm{Se}_x$), the SDW with a modulation $Q_m = (\pi, 0)/(0, \pi)$ has been argued to lead to a CDW with $Q_c = 2Q_s$.[10] The phenomenology also extends to the "hidden-order" state of heavy fermion $\mathrm{URu}_2\mathrm{Si}_2$ which has an incommensurate modulation at $Q_h = (0.6\pi, 0)/(0, 0.6\pi)$ and the formation of the CDW at $Q_c = 2Q_h$ has been predicted.[11] It is thus timely and important to investigate the nature of the density wave order of the conventional SC quasiparticles and their coupling to the vacancy order in Fe-selenide as another example of the same basic principle of modulated states high-T_c superconductivity.

The paper is organized as follows. In Sec. II, we present the experimental phase diagram and the crystal and magnetic structure of $A_y\mathrm{Fe}_{2-x/2}\mathrm{Se}_2$. The induction process of magnetic order due to the vacancy order to give rise to a modulated ground state is calculated in Sec. III. The compatibility of d-wave superconductivity with the presence of vacancy order is discussed in terms of crystal and orbital symmetry in Sec. IV. Finally, we conclude in Sec. V.

II. PHASE DIAGRAM

Fig. 1(a) gives the experimental phase diagram[1] as a function of temperature and Fe vacancy for $A_y\mathrm{Fe}_{2-x/2}\mathrm{Se}_2$. The relationship between y and x compositions is not well established yet, although some experiments suggest that $y \approx x$ for most of these materials.[1] Our calculations consistently demonstrate that the vacancy order in Fe-selenide at a superlattice modulation of $\mathbf{Q}_v = (\frac{1}{5}, \frac{3}{5})$ (Refs. 12 and 13) breaks the translational symmetry of the tetragonal crystal in such a way that it induces structural, magnetic, and unconventional SC phase transition exactly at the same value of $x \sim 0.87$. At the vacancy order transition temperature $T_v \simeq 578$ K in $\mathrm{K}_{0.82(2)}\mathrm{Fe}_{1.626(3)}\mathrm{Se}_2$ (Ref. 2), the crystal structure undergoes a transition from the high-temperature tetragonal $\mathrm{BaFe}_2\mathrm{As}_2$-like structure of $I4/mmm$ space group to a lower symmetry tetragonal structure of $I4/m$ where the latter can be understood as a $\sqrt{5} \times \sqrt{5} \times 1$ superlattice of the former; see Fig. 1(b). Subsequently, a block checkerboardlike antiferromagnetic (AFM) order stabilized with significantly enhanced moments on the Fe sites [about 3.3 μ_B] below a Néel temperature $T_N \approx 559$ K$< T_v$ with an order vector $\mathbf{Q}_m = (\frac{4}{5}, \frac{2}{5})$.[2] Finally,
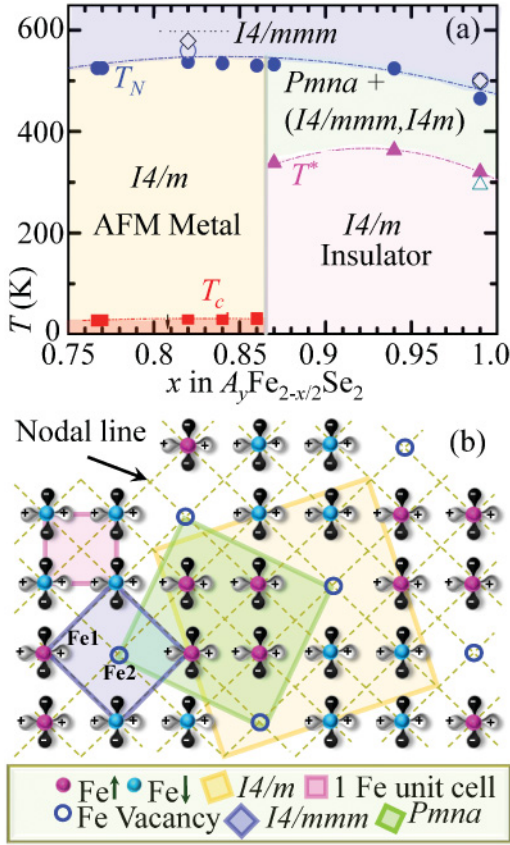
FIG. 1. (Color online) (a) Experimental phase diagram of $A_y Fe_{2-x/2}Se_2$ compound taken from Ref. 1 is also shown to be a common phase diagram for this class of materials $A_y Fe_{2-x/2}Se_2$ in Ref. 12. At high temperature, the system is in the $Ba_2 Fe_2 As_2$-like tetragonal structure of $I4/mmm$ space group at all Fe vacancies. A tetragonal structure with an $I4/m$ unit cell is observed to stabilize at low temperature in the $\sqrt{5} \times \sqrt{5} \times 1$ superlattice. The metal-insulator transition is observed at $x \sim 0.865$ in numerous experiments albeit a smooth behavior of the Néel temperature T_N (diamond) throughout the phase diagram. The open diamond symbol marks the transition temperature at which the disorder-to-order state of the Fe vacancy is measured. Solid squares represent $T_c \sim 30$ K, which seems to be symmetric around $x = 0.8$ at which full occupancy of Fe2 sublattices and vacant Fe1 sites is realized. (b) Corresponding common crystal and magnetic structure in the real space tetragonal $I4/m$ unit cell (top view) in which only Fe atoms are shown (Refs. 1,2, and 12). Magenta and cyan color circles give spin-up and spin-down configurations, while black and white dumbbells represent positive and negative phase of the pairing symmetry. Boxes of different colors and sizes stand for different unit cells (see text), while the gold box is the true unit cell for this system at low temperature.

superconductivity appears below $T_c \simeq 32$ K. Later on this overall phenomena has been observed to be a common feature in all iron-selenide chalcogenides studied so far.[1,12]

III. VACANCY ORDER AND MAGNETIC ORDER

We concentrate here on a particular case of $K_{0.82(2)}Fe_{1.626(3)}Se_2$ at which the vacancy superstructure and

the magnetic structure have propagation vectors $\mathbf{Q}_v = (\frac{1}{5}, \frac{3}{5})$ and $\mathbf{Q}_m = (\frac{4}{5}, \frac{2}{5})$ (Ref. 2). The property of the magnetic order $Q_m = 4Q_v$ motivates us to provide a modulated order model in which the vacancy order is the driving instability which induces the magnetic order at $T_N < T_v$. Vacancy order will naturally develop a CDW at $2Q_v$. Neutron and x-ray study in a Cs-intercalated compound $Cs_y Ke_{2-x/2}Se_2$ showed the presence of the superstructure reflection at $Q = (\frac{2}{5}, \frac{1}{5})$ (Ref. 14) which is equal to $2Q_v$ (antiphase). Finally, the vacancy order clearly breaks the rotational C_4 symmetry of the crystal, leading to a global nematic order parameter. The unidirectional nematic order breaks the t_{2g} symmetry of the Fe d orbitals (which contribute mostly to the bands near the Fermi level) and thus an orbital order around each vacancy can also be expected. We assume the orbital order will have modulation at $3Q_v$. Such an induction process is reversible as long as the modulation vector is incommensurate, which we assume to be the case. It is interesting to note that such possible nematic order is consistent with claims of nematicity in cuprates,[7] pnictide,[10] URu_2Si_2,[11,15] and $Sr_3Ru_2O_7$,[16] although the details of the ordering are material sensitive.

The coupling between the modulated order with d-wave superconductivity is strongly constrained by symmetry and momentum conservations and belongs to a point-group symmetry. Due to C_4 symmetry breaking, s-wave and d-wave representations always mix, but $d_{x^2-y^2}$ and d_{xy} pairing remain clearly distinguishable.[7,17] Therefore, the order parameter can be defined globally via the electronic momentum distributions as $\phi_g = \sum_{\mathbf{k}} d_{\mathbf{k}} \langle c^\dagger_{\mathbf{k}',\alpha} \Sigma_{\alpha,\beta} c_{\mathbf{k}\beta} \rangle$, where $d_{\mathbf{k}}$ is the structure factor for various d waves and $\Sigma_{\alpha,\beta} = \delta_{\alpha,\beta}$ or $\sigma_{\alpha,\beta}$ for scalar and vector orders, respectively. Decoupling the global parameter into the local orders, one can acquire well-defined directions as $\phi_i = \sum_{\mathbf{k},\sigma} \langle c^\dagger_{\mathbf{k}+\mathbf{Q}_i\sigma} c_{\mathbf{k}\sigma} \rangle$ for scalar or $\phi_i = \sum_{\mathbf{k},\sigma} \langle c^\dagger_{\mathbf{k}+\mathbf{Q}_i\uparrow} c_{\mathbf{k}\downarrow} \rangle$ for spin orders. Similarly for superconductivity, we obtain modulated orders $\psi_i = \sum_{\mathbf{k}} \langle c^\dagger_{\mathbf{k}+\mathbf{Q}_i\uparrow} c^\dagger_{-\mathbf{k}\downarrow} \rangle$, while the zero-momentum SC order parameter is $\psi_0 = \sum_{\mathbf{k}} \langle c^\dagger_{\mathbf{k}\uparrow} c^\dagger_{-\mathbf{k}\downarrow} \rangle$. Here, we restrict ourselves to a case with $i = 1$–4: $i = 1$ for vacancy order, $i = 2$ for charge order, $i = 3$ for orbital order, and $i = 4$ for magnetic order. Keeping only the linear terms in the global modulated order parameter ϕ_n in the tetragonal crystal environment, we can write all the coupling terms as[7]

$$\phi_g \sum_{i=1}^{4} \lambda_i |\phi_{i\alpha}|^2 + \phi_1^* \sum_{i=2}^{4} \lambda_{1i} \phi_1^* \phi_i + \sum_{i=1}^{n} \left[\lambda_0^s \phi_1^* \psi_i \bar{\psi}_i^* \right.$$
$$\left. + \lambda_i^s (\phi_1^* \psi_0 \psi_i^* + \phi_1 \psi_0 \bar{\psi}_i^*) \dots + c.c \right]. \quad (1)$$

The coupling constants λ_{1i} between vacancy order with others are possible only if the corresponding modulation follows: $\mathbf{Q}_i = n\mathbf{Q}_1$ relation ($\mathbf{Q}_1 = \mathbf{Q}_v$). We will comment on the superconductivity below.

In Fig. 2, we show the evolution of the FS reconstruction and the nature of the gap opening in the normal state. Absorbing the coupling constant in the order parameters, we define the mean-field gaps as $V_i (= \lambda_i \phi_i)$. The eigenvector is $\Psi_0^\dagger = (c^\dagger_{\mathbf{k}\sigma} c^\dagger_{\mathbf{k}+\mathbf{Q}_1\sigma} c^\dagger_{\mathbf{k}+\mathbf{Q}_2\sigma} \dots)$, where $c^\dagger_{\mathbf{k}+\mathbf{Q}_1\sigma}$ is the creation operator for the Q_1th order and so on. We construct the two-band model Hamiltonian in the 2-Fe unit cell in the normal

state (i.e., when SC order parameters ψ_0 and ψ vanish) as

$$H_0 = \Psi_0^\dagger(\mathbf{k}) \begin{pmatrix} \xi_{\mathbf{k}}^{11} & \xi_{\mathbf{k}}^{12} & V_v & 0 & V_2 & 0 & V_3 & 0 & V_m & 0 & \dots & V_m & 0 & V_3 & 0 & V_2 & 0 & V_v & 0 \\ \xi_{\mathbf{k}}^{21} & \xi_{\mathbf{k}}^{22} & 0 & V_v & 0 & V_2 & 0 & V_3 & 0 & V_m & \dots & 0 & V_m & 0 & V_3 & 0 & V_2 & 0 & V_v \\ V_v^* & 0 & \xi_{\mathbf{k}+\mathbf{Q}}^{11} & \xi_{\mathbf{k}+\mathbf{Q}}^{12} & V_v & 0 & V_2 & 0 & V_3 & 0 & \dots & 0 & 0 & V_m & 0 & V_3 & 0 & V_2 & 0 \\ 0 & V_v^* & \xi_{\mathbf{k}+\mathbf{Q}}^{21} & \xi_{\mathbf{k}+\mathbf{Q}}^{22} & 0 & V_v & 0 & V_2 & 0 & V_3 & \dots & 0 & 0 & 0 & V_m & 0 & V_3 & 0 & V_2 \\ \vdots & \vdots & \vdots & \vdots & \vdots & \vdots & \vdots & \vdots & \vdots & \vdots & \ddots & \vdots & \vdots & \vdots & \vdots & \vdots & \vdots & \vdots & \vdots \\ V_v^* & 0 & V_2^* & 0 & V_3^* & 0 & V_m^* & 0 & 0 & 0 & \dots & V_3^* & 0 & V_2^* & 0 & V_v^* & 0 & \xi_{\mathbf{k}+9\mathbf{Q}}^{11} & \xi_{\mathbf{k}+9\mathbf{Q}}^{12} \\ 0 & V_v^* & 0 & V_2^* & 0 & V_3^* & 0 & V_m^* & 0 & 0 & \dots & 0 & V_3^* & 0 & V_2^* & 0 & V_v^* & \xi_{\mathbf{k}+9\mathbf{Q}}^{21} & \xi_{\mathbf{k}+9\mathbf{Q}}^{22} \end{pmatrix} \Psi_0(\mathbf{k}). \quad (2)$$

The bare dispersion, ξ_k, matrix arises from two tight-binding bands of strongly hybridized t_{2g} orbitals present near the Fermi level.[18] In such an incommensurate case, the FS reconstruction is determined by multiple translations of the bare band structure $\xi_{\mathbf{k}}$ by $\pm n\mathbf{Q}_v$, where the largest value of the integer n is determined by $\mathbf{Q}_v = (2\pi, 2\pi)$ in 2D which is 10 in our case. Each component of the translated dispersion is denoted
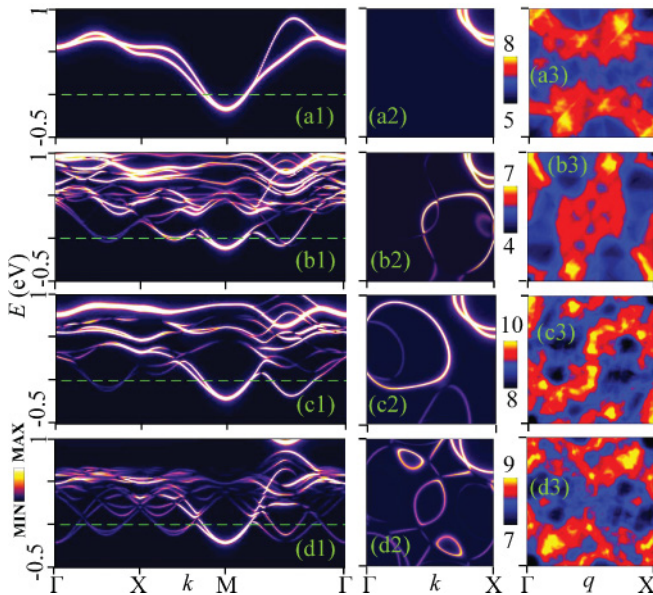

FIG. 2. (Color online) The band dispersion along high-symmetry lines [(a1),(b1),(c1),(d1)], corresponding FSs [(a2),(b2),(c2),(d2)] and bare susceptibility [(a3),(b3),(c3),(d3)] maps at zero energy are presented for four combinations of interactions: (a) → all $V_i = 0$, (b) → only $V_v = -0.5$ eV, (c) → only $V_m = 0.02$ eV, and (d) → $V_v = -0.5, V_2 = 0.2, V_3 = -0.1, V_m = 0.01$ eV. FS and susceptibility are plotted only in the first quadrant of the BZ which are symmetric in the other quadrants. Note that opposite phases between consecutive interactions give maximal weight on main bands. The electronic structure consists of 20 split bands while the spectral weight is largest in the main band if coherence factors of the modulated order are included. Here we have not included the structure factor of the modulated orders which may further enhance the distribution of the spectral weight among the modulated bands.

by $\xi_{\mathbf{k}+n\mathbf{Q}}$. As in the case of non-SC Cr,[4] cuprate,[17] or other SC materials,[10,11,15,16] incommensurability causes hierarchy of gap openings of order $\Delta_m^{v,v'} \sim (V_v^{vm}/W^{m-1} + V_v^{v'm}/W^{m-1})$ (W is bare band width, Δ should not be confused with SC gap) at band crossings between $\xi_{\mathbf{k}+n\mathbf{Q}}^v$ and $\xi_{\mathbf{k}+(n\pm m)\mathbf{Q}}^{v'}$.[19] As long as $V_i \ll W$, the FS is well described by including the lowest-order gap only, and we will neglect all the matrix elements with $m > 1$ and the momentum dependence in the potential V_i.

We have used the eigenstates and eigenvectors of Eq. (2) to compute the band dispersion along high-symmetry lines and the corresponding FS in the normal state, as shown in Fig. 2. The results are presented for various V_i, while fixing the number of quasiparticles on the FS. We also present the real part of the noninteracting static susceptibility χ in the 2D q space calculated from the Hamiltonian in Eq. (2). The present susceptibility calculations do not include any overlap of matrix-element effects.[20]

To understand the evolution of the modulated order due to turning on of individual interactions, it is useful to examine them first separately. In the nonordered state (all $V_i = 0$), the FS consists of two electron-like closed orbits centering at M point in the 2-Fe unit cell, see Figs. 2(a1) and 2(a2). The corresponding susceptibility in Fig. 2(a3) shows nesting peaks or streaks at all nQ_v's, while the intensity dominates at Q_v and $Q_m = 4Q_v$. With the turning on of $V_v = -0.5$ eV, the vacancy order is illuminated and the FS reconstruction becomes complicated, see Fig. 2(b). Both electron pockets are still present in closed orbits, but their size and the associated spectral weight are reduced. The missing spectral weight is shared by a newly developed electron pocket and several open orbit FS pieces. The phase of the interaction V_v does not have significant effect on the modulated pattern (not shown).

We now study the magnetic ordering in Fig. 2(c). To connect the magnetic order parameter V_m with experiments, we will investigate local moments. Neutron diffraction has determined a large magnetic moment block checkerboard AFM in the range 2.3–3.3 μ_B per Fe atom for all known iron-selenide superconductors.[2,12] Within our mean-field approach, we find that a value of $V_m = 20$ meV produces maximal local moments of $2\mu_B\langle S_z\rangle_{\max} \approx 0.12\,\mu_B$ in the 2-Fe unit cell which is smaller than seen in experiments. The value of computed magnetic moments can be enhanced by various modifications

of our calculation, e.g., when all d orbitals are included. With all interactions included, a drastic band folding and FS reconstruction are observed in Fig. 2(d). The corresponding susceptibility continues to exhibit dominant nesting along the vacancy order vector. First-principle calculations have demonstrated drastic FS reconstruction driven by the Fe vacancy and AFM order.[21] Such a FS reconstruction is consistent with observations such as transmission electron microscopy (TEM),[13] NMR,[22] neutron diffraction,[2] and optical studies.[23]

IV. VACANCY ORDER AND d-WAVE PAIRING

As superconductivity turns on, the coupling between the competing order to SC λ_i^s in Eq. (1) is allowed only

when $\mathbf{Q}_1 = i\mathbf{Q}_s$ where $i = 1, 2, \ldots$ ($\mathbf{Q}_s$ is the SC ordering vector in the pair-density channel). Interestingly, the zero-momentum condensate $\mathbf{Q}_s = 0$ is always a complimentary component of the SC state, whereas the finite momentum components are subject to the higher order coupling strength and depend on the nature of the driving instability vector $\mathbf{Q}_1$. Note that λ_1^s alone generates a Fulde-Ferrell-Larkin-Ovchinnikov state. The finite-momentum pairing is also proposed and/or observed in cuprates,[7] URu_2Si_2,[11,15] and $Sr_3Ru_2O_7$,[16] as well as in the organic superconductor κ-$(BEDT\text{-}TTF)_2Cu(NCS)_2$ [BEDT-TTF = Bis(ethylendithiolo) tetrathiofulvalen].[24]

Absorbing the coupling constants λ_i^s in the order parameter, we define the SC gaps as $\Delta_i = \lambda_i^s \psi_i$. Similar to Eq. (2), we can construct the SC gap matrix

$$H_{SC} = \Psi_0(\mathbf{k}) \begin{pmatrix} \Delta_{\mathbf{k}} & 0 & \Delta_{\mathbf{k+Q}} & 0 & \Delta_{\mathbf{k+2Q}} & 0 & \Delta_{\mathbf{k+3Q}} & 0 & \Delta_{\mathbf{k+4Q}} & 0 & \ldots \\ 0 & \Delta_{\mathbf{k}} & 0 & \Delta_{\mathbf{k+Q}} & 0 & \Delta_{\mathbf{k+2Q}} & 0 & \Delta_{\mathbf{k+3Q}} & 0 & \Delta_{\mathbf{k+4Q}} & \ldots \\ \Delta_{\mathbf{k+Q}} & 0 & \Delta_{\mathbf{k}} & 0 & \Delta_{\mathbf{k+Q}} & 0 & \Delta_{\mathbf{k+2Q}} & 0 & \Delta_{\mathbf{k+3Q}} & 0 & \ldots \\ 0 & \Delta_{\mathbf{k+Q}} & 0 & \Delta_{\mathbf{k}} & 0 & \Delta_{\mathbf{k+Q}} & 0 & \Delta_{\mathbf{k+2Q}} & 0 & \Delta_{\mathbf{k+3Q}} & \ldots \\ \vdots & \vdots & \vdots & \vdots & \vdots & \vdots & \vdots & \vdots & \vdots & \vdots & \ddots \end{pmatrix} \Psi_0(-\mathbf{k}). \quad (3)$$

In the Nambu space, we get the modulated SC Hamiltonian as

$$H = \Psi^\dagger \begin{pmatrix} H_0(\mathbf{k}) & H_{SC}(\mathbf{k}) \\ H_{SC}^*(-\mathbf{k}) & H_0(-\mathbf{k}) \end{pmatrix} \Psi. \quad (4)$$

A. Pairing symmetry transformation

The pairing symmetry in these materials without a hole pocket at Γ in the conventional $BaFe_2As_2$-like crystal structure is nodeless and isotropic.[18,25,26] In the rest of the paper, we discuss how the vacancy order plays an important role in the onset of d-wave superconductivity. It has been argued that the d-wave order breaks the translational symmetry.[18,27] To elucidate this, we recall first the example of the $BaFe_2As_2$ pnictide superconductor which hosts both hole and electron pockets at Γ and M points, respectively, in the 2-Fe unit cell and how $s^\pm$-pairing is compatible with the corresponding crystal symmetry. We illustrate this with the help of the unitary transformation from the 1-Fe unit cell to the 2-Fe unit cell where one expects, by construction, to retain all observable such as nodeless SC gap(s) and FS nesting to be compatible with the actual crystal symmetry irrespective of the conventional one used for calculations.

We define a quantity in the 2-Fe unit cell by tilde. The unitary transformation consists of a $45°$ rotation of the crystal with lattice constant $\tilde{a} \to \sqrt{2}a$ which gives $\tilde{k}_{x/y} = (k_x \pm k_y)/2$.[28] In doing so, the $s^\pm$ pairing in the 2-Fe unit cell becomes a $\tilde{s}_{xy}$-like symmetry in the 1-Fe unit cell in which two inequivalent Fe sites possess opposite phases in real space, see Figs. 3(a)–3(c). In momentum space, the SC gap symmetry is compatible with the FS topology. In real space, the gap phase
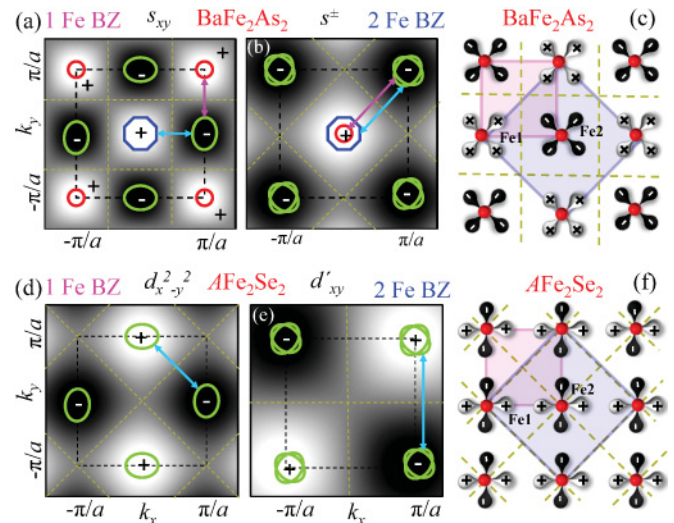

FIG. 3. (Color online) Schematic behavior of the FS and pairing symmetry in 1 Fe per unit cell and 2 Fe per unit cell Brillouin zone for $BaFe_2As_2$ are shown in (a) and (b), respectively. The corresponding real-space view of the gap symmetry is depicted in (c) in which the SC phase is isotropic and nodeless on each Fe atom but changes phase between Fe1 and Fe2 sublattices. Black to white color scale depicts the pairing symmetry from negative to positive in momentum space while black and white dumbbells represent the negative and positive phase of the pairing symmetry in real space (exponential form of cosine and sine functions). Similar results for AFe_2Se_2 compounds are given in (d)–(f). In momentum space FSs are isotropic and nodeless, but in real space the gap nodes pass through both of the Fe atoms. The phases of the pairing symmetries are $s_{xy} = 2\cos(k_x a)\cos(k_y a)$, $s^\pm/d_{x^2-y^2} = \cos(k_x a) \pm \cos(k_y a)$, and $d'_{xy} = 2\sin(k_x a)\sin(k_y a)$.

obeys proper translational symmetry in the true 2-Fe unit cell, but not in the 1-Fe unit cell (conventional). This seems to pose a problem that is in fact an artificial issue. A proper unit cell contains 2 inequivalent Fe sites; the 1-Fe unit cell is an artificial one constructed for convenience of calculations assuming 2 inequivalent Fe to be the same.

We now look at the SC gap transformation. As obvious in pnictide, the sign change of the SC gap in $s^{\pm}$ pairing occurs between Fe1 and Fe2 atoms, see Fig. 3(c). Therefore, when the center Fe2 atom is removed from the lattice (when vacancies are present and ordered) in $A_y\text{Fe}_{2-x/2}\text{Se}_2$, one can expect a different SC pairing symmetry to obtain sign change in the bulk SC order parameter. All of the Fe1 atoms are now equivalent, the sign change of gap in the pairing function should be carried by all atoms, i.e., a d-wave or p-wave state can arise. In $A_y\text{Fe}_{2-x/2}\text{Se}_2$ compounds when T_c is highest at $x \sim 0.8$, a d-wave gap is a most natural pairing state to arise.[18,25,26] NMR studies also indicate the presence of a spin-singlet pairing channel in the K intercalated samples with different composition.[22] The d-wave pairing which gives rise to a nodeless and nearly isotropic SC gap on the FSs, is also consistent with numerous observables.[18]

On the other hand, the d-wave SC gap in $A_y\text{Fe}_{2-x/2}\text{Se}_2$ compounds has an additional complication. While a $d_{x^2-y^2}$-wave gap is compatible in both momentum and real space of the conventional 1-Fe unit cell, it is inconsistent when the pairing symmetry is transformed to the 2-Fe unit cell. For example, in Fig. 3(e), when a $k = (-\pi, -\pi)$ point is shifted by the reciprocal vector of $(2\pi/a, 0)$ (assuming a square lattice), the FS topology is restored but the SC order maps on the site with an opposite sign of the gap function. We propose that this problem can be cured by doubling the Brillouin zone in the momentum space. One way of doing it is by removing the Fe2 atom from the center of the unit cell in Fig. 3(f). Therefore, a d-wave gap is possible in these compounds when the normal state vacancy order helps restore the translational symmetry of the crystal.

Iron-selenide materials host a SC dome-like feature centering at $x \approx 0.8$ as long as vacancy order persists, see Fig. 1(a).

It has been reported that at $x = 0.8$, all Fe2 atoms from the sublattice are completely removed.[2] This observation is consistent with the symmetry expected for the d-wave pairing. Such a pattern of competing order is forbidden in the 2-Fe 122-pnictide $I4/mmm$ structure,[12] and the system stabilizes to a low-temperature tetragonal $I4/m$ one, as indicated by the yellow box in Fig. 1(b).

V. CONCLUSION

In conclusion, we present a microscopic model to show that the onset of vacancy order leads to many significant modifications of electronic, magnetic, and superconducting properties of iron-selenide superconductors. A block checkerboard AFM state with moments as large as 3.3 μ_B is realized experimentally and is believed to be induced by the vacancy order at $\mathbf{Q}_m = 4\mathbf{Q}_v$. Such a modulated ground state compensates for the broken translational symmetry of the d-wave superconductivity[18] and therefore allows for the state with combined superconductivity and structural modulations to develop. In this state, the superconducting gap is nodeless and nearly isotropic on the FSs, as observed in numerous experiments.

The results follow the same route as in other high-T_c superconductors where a modulated ground state of multiple competing phases promotes and coexists with superconductivity in a uniform phase rather than undergoing any nanoscale phase separation. The modulated superconductivity has also been seen in cuprates,[7,17] pnictides,[10] URu$_2$Si$_2$,[11,15] and Sr$_3$Ru$_2$O$_7$,[16] although the nature of competing phases may vary across these materials.

[1] W. Bao, G. N. Li, Q. Huang, G. F. Chen, J. B. He, M. A. Green, Y. Qiu, D. M. Wang, and J. L. Luo, e-print arXiv:1102.3674.

[2] W. Bao, Q. Huang, G. F. Chen, M. A. Green, D. M. Wang, J. B. He, X. Q. Wang, and Y. Qiu, Chinese Phys. Lett. **28**, 086104 (2011).

[3] J. M. Tranquada, B. J. Sternlieb, J. D. Axe, Y. Nakamura, and S. Uchida, Nature (London) **375**, 561 (1995).

[4] E. Fawcett, Rev. Mod. Phys. **60**, 209 (1988).

[5] W. D. Wise, K. Chatterjee, M. C. Boyer, T. Kondo, T. Takeuchi, H. Ikuta, Zhijun Xu, J. Wen, G. D. Gu, Y. Wang, and E. W. Hudson, Nature Physics **5**, 213 (2009).

[6] T. Das, R. S. Markiewicz, and A. Bansil, Phys. Rev. B **77**, 134516 (2008).

[7] M. Vojta, Adv. Phys. **58**, 699 (2009); E. Berg, E. Fradkin, and S. A. Kivelson, Phys. Rev. B **79**, 064515 (2009).

[8] R. S. Markiewicz, J. Lorenzana, G. Seibold, and A. Bansil, Phys. Rev. B **81**, 014509 (2010).

[9] T. Das, R. S. Markiewicz, and A. Bansil, Phys. Rev. B **81**, 184515 (2010).

[10] A. V. Balatsky, D. N. Basov, and J.-X. Zhu, Phys. Rev. B **82**, 144522 (2010).

[11] J.-J. Su, Y. Dubi, P. Wolfle, and A. V. Balatsky, J. Phys. Condens. Matter **23**, 094214 (2011).

[12] F. Ye, S. Chi, W. Bao, X. F. Wang, J. J. Ying, X. H. Chen, H. D. Wang, C. H. Dong, and M. Fang, e-print arXiv:1102.2882.

[13] Z. Wang, Y. J. Song, H. L. Shi, Z. W. Wang, Z. Chen, H. F. Tian, G. F. Chen, J. G. Guo, H. X. Yang, and J. Q. Li, Phys. Rev. B **83**, 140505(R) (2011).

[14] V. Yu. Pomjakushin, D. V. Sheptyakov, E. V. Pomjakushina, A. Krzton-Maziopa, K. Conder, D. Chernyshov,

V. Svitlyk, and Z. Shermadini, Phys. Rev. B **83**, 144410 (2011).

[15] C. M. Varma and L. Zhu, Phys. Rev. Lett. **96**, 036405 (2006).

[16] R. A. Borzi, S. A. Grigera, J. Farrell, R. S. Perry, S. J. S. Lister, S. L. Lee, D. A. Tennant, Y. Maeno, and A. P. Mackenzie, Science **315**, 214 (2007).

[17] A. J. Millis and M. R. Norman, Phys. Rev. B **76**, 220503(R) (2007); N. Harrison, Phys. Rev. Lett. **102**, 206405 (2009); A. Hackl, M. Vojta, and S. Sachdev, Phys. Rev. B **81**, 045102 (2010).

[18] T. Das and A. V. Balatsky, Phys. Rev. B **84**, 014521 (2011).

[19] We approximate all components of the potentials to be the same for both bands, but neglecting interband components.

[20] T. Das and A. V. Balatsky, Phys. Rev. Lett. **106**, 157004 (2011).

[21] C. Cao and J. Dai, Phys. Rev. Lett. **107**, 056401 (2011); X.-W. Yan, M. Gao, Z.-Yi Lu, and T. Xiang, Phys. Rev. B **83**, 233205 (2011).

[22] W. Yu, L. Ma, J. B. He, D. M. Wang, T.-L. Xia, G. F. Chen, and W. Bao, Phys. Rev. Lett. **106**, 197001 (2011); D. A. Torchetti M. Fu, D. C. Christensen, K. J. Nelson, T. Imai, H. C. Lei, and C. Petrovic, Phys. Rev. B **83**, 104508 (2011).

[23] Z. G. Chen *et al.*, Phys. Rev. B **83**, 220507(R) (2011).

[24] M. Salmhofer, C. Honerkamp, W. Metzner, and O. Lauscher, Prog. Theor. Phys. **112**, 943 (2004).

[25] T. A. Maier, S. Graser, P. J. Hirschfeld, and D. J. Scalapino, Phys. Rev. B **83**, 100515(R) (2011).

[26] Fa Wang, F. Yang, M. Gao, Z.-Yi Lu, T. Xiang, and D.-H. Lee, Europhy. Lett. **93**, 57003 (2011).

[27] I. I. Mazin, Physics **4**, 26 (2011); Phys. Rev. B **84**, 024529 (2011).

[28] Such a unitary transformation is exact if two inequivalent Fe atoms become in-plane, otherwise it is an approximation. Such an approximation is reasonable as long as the FS and gap symmetry are quasi-two-dimensional as in the present case.